Structural Characterization of Monellin in the Alcohol-Denatured State by NMR: Evidence for β-Sheet to α-Helix Conversion†

Pei Fan, Clay Bracken, and Jean Baum*

Department of Chemistry, Rutgers University, Piscataway, New Jersey 08854-0939

Received August 21, 1992; Revised Manuscript Received November 30, 1992

ABSTRACT: Two-dimensional ^{1}H NMR spectroscopy and hydrogen exchange methods have been used to characterize the alcohol-denatured state of monellin. Monellin is a sweet tasting protein composed of two chains. In the native state, the A-chain consists entirely of β-structure, and the B-chain contains both α- and β-structure. Upon addition of either 50% ethanol or 50% trifluoroethanol (TFE), the native structure of monellin is disrupted resulting in an alcohol-denatured state with properties different from those of the random coil state. In the alcohol-denatured state, the far-UV circular dichrosim (CD) spectrum displays a higher helical content relative to the native state and the intensity of the near-UV CD signal is completely lost. One-dimensional NMR studies show that there are approximately 14 amide protons protected from exchange with solvent in the alcohol-denatured state and that large portions of the protein exchange at a rate that is comparable to the exchange rate of the protein in urea. Utilizing hydrogen exchange trapping techniques, the slowly exchanging residues are identified at pH 2.0 in 50% ethanol and 50% TFE (A10–A15, A18, A19, A21, A24, and A39) and are found to be clustered on one region of the A-chain. Preliminary 2D NMR assignments show that in the alcohol-denatured state the A-chain of monellin undergoes structural reorganization, with one strand of the native state β-sheet on the A-chain (residues A17–A30) becoming an α-helix in the alcohol-denatured state. The secondary structure of the A-chain in the alcohol-denatured state is different from the native state structure, although the slowly exchanging residues are similar.

To understand how and when different forces come into play to direct protein folding, the study of folding intermediates and denatured states has fundamental importance (Dill & Shortle, 1991). Intermediate and denatured states of proteins, due to their transient and/or dynamic nature, are not as easily studied as native states of proteins. However, with the combination of hydrogen exchange techniques and multidimensional NMR,[1] an increasing amount of structural information has been obtained about transient and stable folding intermediates of proteins (Udgaonkar & Baldwin, 1988; Roder et al., 1988; Bycroft et al. 1990; Radford et al., 1992a; Briggs & Roder, 1992). Using these techniques, several molten globule proteins and partially folded states of proteins have been characterized at the individual residue level (Baum et al., 1989; Hughson et al, 1990; Jeng et al., 1990; Jeng & Englander, 1991; Harding et al., 1991; Alexandrescu et al., 1993; C-L. Chyan, C. Wormald, C. M. Dobson, P. A. Evans, and J. Baum, unpublished results). Information concerning the structure of denatured states of proteins is still very limited, although hydrogen exchange kinetics and assignments of thermally unfolded proteins and urea-denatured proteins have recently become available (Evans et al., 1991; Robertson & Baldwin, 1991; Neri et al., 1992; Radford et al., 1992b). Denatured states of proteins can be obtained either thermally or chemically, with guanidine and urea being the most commonly used chemical denaturants. An alternative denatured state can be obtained by placing proteins in alcohols. Short-chain alcohols, such as methanol, ethanol, propanol, and trifluoroethanol, can disrupt the native state of proteins and induce secondary structure, in particular α-helices (Timasheff et al., 1966; Tanford, 1968; Timasheff & Inoue, 1968; Arakawa & Goddette, 1985). Structural studies of the alcohol-denatured state and comparison of the structure with that of the native form are important in order to understand how secondary structure depends on the environment in which an amino acid sequence is found.

Monellin is an intensely sweet protein of 95 residues isolated from the berries of *Dioscoreophyllum cumminsii* (Morris & Cagan, 1972). The protein is composed of two noncovalently bound dissimilar subunits, the A-chain of 45 residues and the B-chain of 50 residues (Hudson & Biemann, 1976; Frank & Zuber, 1976). The X-ray crystal structure has been determined (Ogata et al., 1987), and a backbone diagram is shown in Figure 1. There is a five-stranded antiparallel β-sheet composed of three strands from the A-chain and two strands from the B-chain. An α-helix of 15 residues is located on the B-chain and runs almost perpendicular to the β-sheet. No disulfide bond is present in monellin, and the two chains appear to be held together predominantly by interchain hydrophobic interactions with additional contributions from hydrogen bonding and salt bridging. Monellin remains in the native state throughout the pH range 1–10 at room temperature and is fairly resistant to heat denaturation at neutral pH (T_m > 80 °C) (Kim et al., 1989). Previous CD studies of monellin indicate that the protein retains its native conformation in 25% ethanol, exhibiting ~6–10% helix content, whereas in 50% ethanol, the native structure is disrupted and the protein undergoes a reorganization to a higher helical content (Jirgenson, 1976). Our interest in nonnative state protein characterization led us to examine the alcohol-denatured state of monellin in further detail. The protein is particularly suitable for NMR analysis, as it is highly structured, containing both α-helix and β-sheet, and does not contain any disulfide

† This work was supported by the Searle Scholar Fund/Chicago Community Trust.

* To whom correspondence should be addressed.

[1] Abbreviations: NMR, nuclear magnetic resonance; 1D, one dimensional; 2D, two dimensional; CD, circular dichroism; DQF-COSY, double-quantum filtered correlation spectroscopy; NOE, nuclear Overhauser enhancement; NOESY, nuclear Overhauser enhancement spectroscopy; TOCSY, total correlation spectroscopy; UV, ultraviolet; TFE, trifluoroethanol; TFA, trifluoroacetic acid.

0006-2960/93/0432-1573$04.00/0 © 1993 American Chemical Society

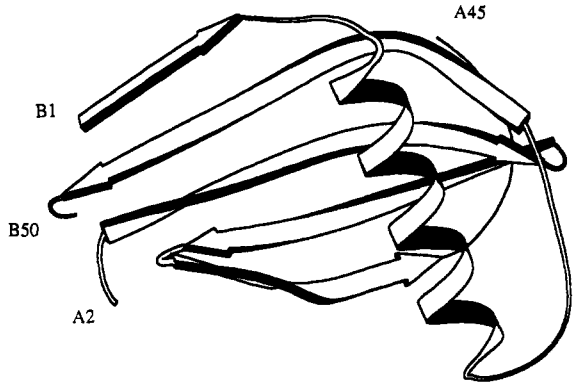

	A1	A5	A10	A15	A20
A chain	Phe Arg Glu Ile Lys Gly Tyr Glu Tyr Gln Leu Tyr Val Tyr Ala Ser Asp Lys Leu Phe				
	A25	A30	A35	A40	
	Arg Ala Asp Ile Ser Glu Asp Tyr Lys Thr Arg Gly Arg Lys Leu Leu Arg Phe Asn Gly				
	A45				
	Pro Val Pro Pro Pro				

	B1	B5	B10	B15	B20
B chain	Gly Glu Trp Glu Ile Ile Asp Ile Gly Pro Phe Thr Gln Asn Leu Gly Lys Phe Ala Val				
	B25	B30	B35	B40	
	Asp Glu Glu Asn Lys Ile Gly Gln Tyr Gly Arg Leu Thr Phe Asn Lys Val Ile Arg Pro				
	B45	B50			
	Cys Met Lys Lys Thr Ile Tyr Glu Asn Glu				

FIGURE 1: Ribbon diagram of monellin based on the crystal structure (Ogata et al., 1987). The primary sequence of monellin is shown below.

bonds. We set out to determine, at the individual residue level, where the changes occur in this alcohol-denatured state and the relative regions of stability in the reorganized structure.

In this paper, we describe the detailed structural characterization of monellin in 50% ethanol and 50% TFE solutions using NMR spectroscopy. Bulk hydrogen exchange methods and hydrogen exchange methods that involve amide trapping are used to locate the slowly exchanging amide protons and to describe the dynamics of the alcohol-denatured state. In addition, we capitalize on the fact that the chemical shift dispersion of the denatured state of monellin in TFE is larger than the chemical shift dispersion of most aqueous denatured states. This allows us to obtain direct sequential assignments by 2D NMR methods and to deduce regions of protein secondary structure. Hydrogen exchange kinetics obtained via trapping techniques and secondary structure obtained by direct assignment provide a picture of the alcohol-denatured state. In addition, the structure and hydrogen exchange patterns of the alcohol-denatured state are compared to the native state to determine how the environment of the protein affects secondary structure formation.

MATERIALS AND METHODS

Monellin was purchased from Sigma Chemical Co. Deuterium oxide (99.9% deuterated) was obtained from Aldrich; deuterated ethanol and trifluoroethanol were obtained from Cambridge Isotope Labs. Monellin was purified using Sephadex CM-25 gel equilibrated in 10 mM phosphate buffer at pH 7.2. Sigma monellin was bound, washed, and then eluted with 100 mM NaCl, 10 mM phosphate buffer (Sung-Hou Kim, private communication). The concentration of monellin was determined using the extinction coefficient $\epsilon_{277nm} = 1.46 \times 10^4\ M^{-1}\ cm^{-1}$ (Morris & Cagan, 1980). The A- and B-chains of monellin were separated by C-18 reverse-phase chromatography using a gradient of 30% methanol, 0.1% TFA to 70% methanol, 0.1% TFA. The separate chains were confirmed by N-terminal amino acid sequencing and mass spectroscopy. The concentrations for each chain were determined by UV absorbance using a calculated extinction coefficient on the basis of the aromatic absorbance at 280 nm (Edelhoch, 1967).

Size-exclusion chromatography was used to determine if the A- and B-chains of monellin are associated/aggregated in alcohol. Samples were dissolved in 100 μL of 50% ethanol, 100 mM NaCl at pH 2.0 and applied to a 1 × 54 cm column packed with Sephacryl S-100HR gel filtration media equilibrated in the same buffer. The total elution time for each column was 6 h. The use of 100 mM NaCl was necessary for eliminating all ionic interactions between the protein and the gel.

Bulk hydrogen exchange experiments, to monitor amide proton disappearance, were recorded using 1D NMR spectroscopy. The exchange experiments were carried out at 25 °C. The protein was dissolved in a solvent mixture (v/v) that was preadjusted to pH 2.0, and after dissolution, the solution pH was quickly readjusted again to 2.0. The pH was not corrected for solvent effects. Sample concentrations ranged from 0.28 mM to 1.15 mM. Acquisition of 1D NMR spectra started typically about 5 min after sample dissolution. The number of amide protons remaining at different time intervals was determined by integrating the intensity of the amide protons and then normalizing to the integrated intensity of the aromatic protons. The hydrogen exchange data were fit using a nonlinear least-squares method. The Marquardt–Levenberg algorithm (Press et al., 1986) was used to minimize the R value which is the sum of squared differences between the experimental value and the calculated value using exponential functions. The minimum number of exponential functions that provide the best R value and the best fit by visual inspection is three.

The hydrogen exchange kinetics of individual amide protons in the alcohol-denatured state were measured by hydrogen exchange trapping methods. The protocol was as follows: first, the protein (typically at a concentration of ~0.7 mM) was dissolved in 50% ethanol-d_6/50% D_2O solution (v/v) or 50% TFE-d_3/50% D_2O (v/v) at pH 2.0. Then, after various lengths of time, the protein was restored to the native state by removing the alcohol either by N_2 evaporation or vacuum drying on a Savant speed-vac. Alcohol removal took less than 30 min by either method, and the remaining water was then removed from the sample by lyophilization. Dilution methods were not used because the refolding rate is slow at low pH and low concentration of protein, and competition between refolding and hydrogen exchange may occur and complicate the results. The renatured protein was redissolved in D_2O at pH 2.0 and 25 °C for NMR studies.

NMR experiments were performed on a Varian 500-MHz spectrometer equipped with a SUN computer at Rutgers University. Quadrature detection in the $t1$ dimension was achieved by using either the time-proportional phase incrementation (TPPI) method (Redfield & Kunz, 1975; Marion & Wuthrich, 1983) or the hypercomplex method (Mueller & Ernst, 1979; States et al., 1982). Sixty four scans of 2K complex data points were collected for each of the 512 $t1$ increments of the NOESY (Kumar et al., 1980; Otting et al., 1986) and TOCSY (Braunsweiler & Ernst, 1983; Bax & Davis, 1985) experiments and the 1024 $t1$ increments of the DQF-COSY experiment (Rance et al., 1983). NOESY experiments were carried out with 150-ms, 200-ms, and 250-ms mixing times, and TOCSY experiments were performed using 35-ms, 50-ms, and 60-ms spin-lock mixing times. In H_2O samples a pre-TOSCY sequence (Otting & Wuthrich, 1987) was incorporated into DQF-COSY and NOESY

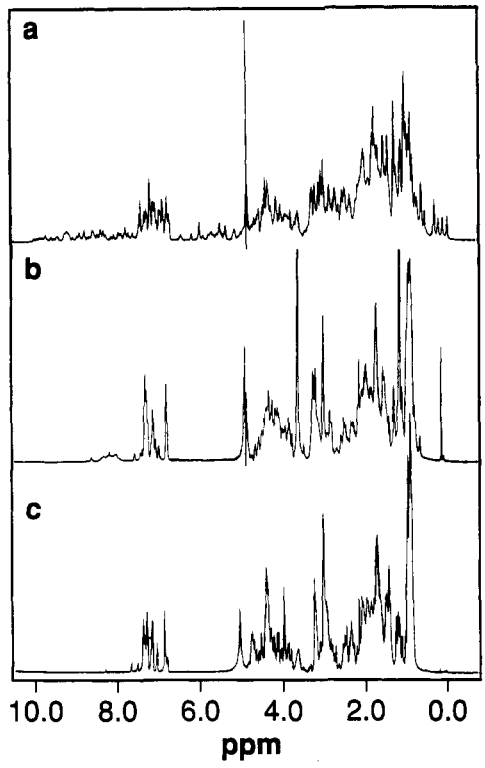

FIGURE 2: 1D ^{1}H NMR spectra of monellin at 25 °C in (a) D_2O at pH 2 (native state); (b) 50% ethanol-d_6/D_2O (alcohol-denatured state); or (c) 9 M urea at pH 2 (unfolded state). In each case, monellin was dissolved in the appropriate solvent and equilibrated for 6 h prior to acquisition of the spectrum.

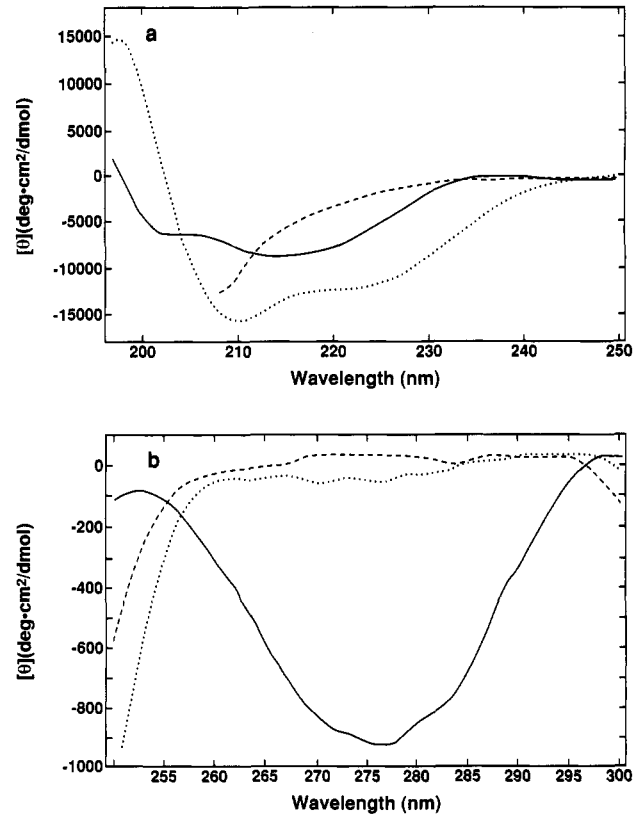

FIGURE 3: CD spectra of monellin recorded at 25 °C in different solvent conditions for the (a) far-UV region (backbone region) and (b) near-UV region (aromatic region). Lines: (—) native state (pH 2); (···) alcohol-denatured state in 50% ethanol at pH 2; (- - -) unfolded state in 9 M urea at pH 2.

experiments with a spin-lock mixing time of 10 ms. All the experimental data were processed on a Silicon Graphics Work Station using FTNMR and FELIX (Hare Research, Inc.). Shifted sine-bell functions were used in both dimensions prior to Fourier transformation.

Circular dichroism experiments were performed on an AVIV circular dichroism spectrometer (Model 60DS). Rectangular cells with path lengths of 0.1, 1, and 10 mm were employed to record the spectrum in both the far-UV (190–250 nm) and near-UV (240–300 nm) regions. Sample concentrations ranged from 2 to 80 μM and spectra were acquired at 25 °C. Deconvolutions of the far-UV CD spectra were carried out using the basis sets of Brahms and Brahms (1980).

RESULTS

1D NMR Spectra of Monellin in Different States. The one-dimensional ^{1}H NMR spectra of monellin in D_2O, in 50% ethanol, and in 9 M urea are presented in Figure 2. The 1D NMR spectrum of monellin in D_2O (Figure 2a) displays substantial chemical shift dispersion and many slowly exchanging amide protons, which are typical for a fully structured protein. The large chemical shift dispersion reflects the different environments of individual residues, and the slowly exchanging amide protons indicate the presence of intramolecular hydrogen bonding and lack of solvent accessibility.

In 9 M urea (Figure 2c), the chemical shift dispersion shown in the native state has disappeared. All the amide protons exchange with D_2O within an hour under this condition, suggesting that the hydrogen bonding interactions in the native state are disrupted. The protein adopts essentially a random coil structure.

The spectrum in 50% ethanol (Figure 2b) is different from both the native and fully unfolded states. The spectrum displays mostly random coil chemical shifts but there are also residues having chemical shifts that differ significantly from random coil values (Wuthrich, 1986). For example, one resonance is shifted to higher field in the aliphatic region. When the temperature of the sample is raised, this resonance moves linearly toward the random coil chemical shift position. Similar temperature-dependent effects are observed for other perturbed resonances, and we note that all of the transitions are linear. From Figure 2b, it is also evident that a group of amide protons are fairly resistant to exchange with the solvent. After 6 h of exposure to 50% ethanol-d_6/D_2O, there is still a significant amount of amide proton intensity left in the NMR spectrum, due to a small set of amide protons that are protected from exchange with the solvent. These facts suggest that although the majority of the protein displays NMR spectra characteristic of random coil or highly dynamical nature, certain parts of the protein still have relatively stable structure and some residues maintained relatively stable hydrogen bonding interactions.

CD Spectra of Monellin in Different States. The CD spectra of monellin in different solvent conditions are shown in Figure 3. Deconvolution of the far-UV CD spectra were accomplished using the basis sets of Brahms and Brahms (1980). In H_2O at pH 2, the far-UV CD indicates that the protein is substantially structured. This is consistent with previous CD observations (Jirgenson, 1976). Using the deconvolution procedure, the native protein is estimated to consist of 8% α-helix, 46% β-sheet, and 46% random coil. The β-sheet content is consistent with what is found in the crystal structure (50%); however, the α-helix content is underestimated (17% in crystal structure). The near-UV CD spectrum of the native protein exhibits a small negative peak around 270 nm due to the aromatic residues, indicating that the aromatic side chains are maintained in a relatively fixed

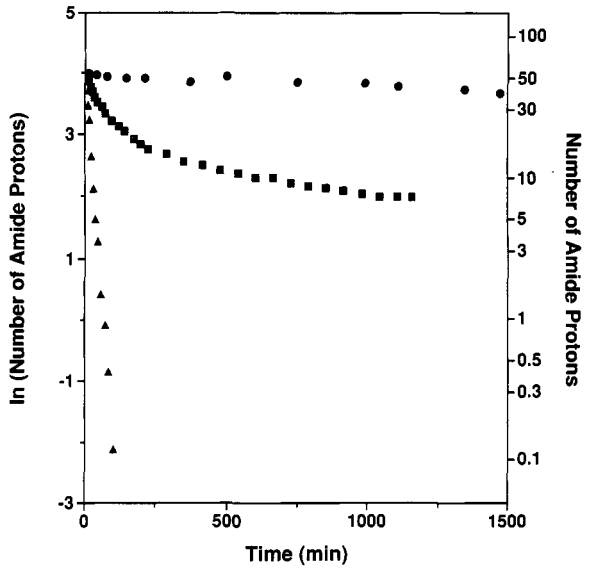

FIGURE 4: Time dependence of the number of unexchanged amide protons of monellin determined by 1D NMR, after sample dissolution in different solvents at 25 °C: (●) in D_2O at pH 2 (native state); (■) in 50% ethanol-d_6/D_2O at pH 2 (alcohol-denatured state); (▲) in 9 M urea at pH 2 (random coil state).

orientation with respect to one another. In 9 M urea at pH 2, the far-UV CD spectrum of monellin shows a significant decrease of secondary structure compared to the native state. We did not attempt to deconvolute the spectrum due to the absence of spectral information below 210 nm which is caused by the intense UV absorption of urea. No CD signal appears in the near-UV region in 9 M urea. In 50% ethanol at pH 2, the CD spectrum shows an increase in the far-UV CD signal compared to that of the native state, and from the deconvolution estimated the structure of the protein to be 58% α-helix, 26% β-sheet, and 16% random coil. However, concomitant with the increase in secondary structure, the tightly packed protein interior is disrupted in 50% ethanol, as evidenced through the loss of intensity of the near-UV CD signal.

Bulk Hydrogen Exchange by 1D NMR. Bulk hydrogen exchange experiments were carried out using 1D NMR. The time-dependent decrease of amide proton intensity of monellin in 50% ethanol is shown in Figure 4. Exchange curves obtained with the native and fully unfolded protein are also shown in the same figure. In the native state at pH 2 the exchange is very slow and is almost invariant on the displayed time scale. However, in 9 M urea the fully unfolded state exchanges very fast, with essentially a simple exponential exchange curve. For the ethanol-denatured state, the exchange curve falls in between that of the native and fully unfolded states. Direct exchange rate comparisons of the different states must be made carefully, because of the different solvents used in each case. In theory, when acid-catalyzed exchange is dominant (pH < 3), change of solvent character should have little effect on the exchange rate. Only under conditions where the exchange is base catalyzed would the presence of ethanol appear to decrease the exchange rate due to suppression of the water dissociation constant by the organic solvent (Englander & Kallenbach, 1984; Gutbezahl & Grunwald, 1953). Therefore, under our experimental conditions (pH 2), qualitative comparisons between the different states can be made.

We have found that the exchange curve for the protein in 50% ethanol can be approximated well by the sum of three exponentials, even though the curve is actually the sum of 90 exponentials corresponding to the number of backbone amide and indole protons in the protein. The fast phase has an amplitude of 16 protons and a rate of 3.8×10^{-2} min^{-1}, the medium phase has 30 amide protons that are ~4 times slower than the fast phase (9.4×10^{-3} min^{-1}), and the slow phase has 14 amide protons that are ~60 times slower than the fast phase (6.7×10^{-4} min^{-1}). The exchange rate observed in urea (6.2×10^{-2} min^{-1}) is slightly faster than that of the fast phase, and urea is known to increase the acid-catalyzed exchange rates in model compounds (Loftus et al., 1986). It should be noted here that there is an additional fast phase with a time constant faster than the dead time of the experiment (typically ~5 min), and this phase includes about 30 amide protons. These data suggest that in 50% ethanol the observed fast and medium exchange phases are likely to arise from the random coil and/or highly dynamic region of the protein. In addition, there is a slow phase containing approximately 14 amide protons which can be associated with the presence of stable structure in the alcohol-denatured state.

Hydrogen Exchange Trapping Experiments. The bulk hydrogen exchange data indicate that certain parts of the protein are very dynamic and that a small subset of protons are slowly exchanging. We are interested in learning, at the individual residue level, the rates of exchange of the amide protons in the alcohol-denatured state. The alcohol-denatured state is difficult to study directly using conventional 2D NMR techniques because of extensive overlap in the NMR spectrum. One way to approach the problem is to perform hydrogen exchange trapping experiments in which the slowly exchanging amide protons in the alcohol-denatured state are probed in the well-resolved spectrum of the native state. These experiments are similar to the trapping experiments that have been used to study partially folded proteins (Baum et al., 1989; Hughson et al., 1990; Jeng et al., 1990; Harding et al., 1991; C. Chyan, C. Hanley, P. Evans, C. M. Dobson, and J. Baum, unpublished results). In the present refolding procedure, the protein was first dissolved in 50% ethanol-d_6/D_2O and then left to exchange with solvent for various periods of time. Afterward, the exchange process was quenched by evaporation of ethanol, and the protein refolded back to its native structure. The ethanol evaporation is a relatively slow process (~30 min), but, during this time period, the solution temperature is low (<10 °C) so the hydrogen exchange rate is slow. In addition, two different renaturation procedures were employed to rule out the possibility of artifacts due to the renaturation method used.

Figure 5 shows the COSY spectra of the fingerprint region of the slowly exchanging amide protons in the native state and the amide protons protected from exchange in 50% ethanol after 6 h. The hydrogen exchange trapping experiments were carried out for 1, 2, 3, 6, and 12 h of exchange times. The exchange profiles of protected amide protons are shown in Figure 6a. Due to the long time that is required for the renaturation process, the data are treated semiquantitatively. A value of 0 is assigned to amide protons that are rapidly exchanging in the native state. A value of 0.5 or greater is assigned to amide protons that are slow to exchange in the native state. Values of 1, 3, 6, and 12 are assigned to the amides that are observed in the native state COSY spectra after 1, 3, 6, and 12 h of exchange in 50% ethanol, respectively. From Figure 6a it can be seen that at short exchange times (≤6 h) the residual amide protons are distributed on both the A- and B-chains of monellin. However, at longer exchange times (>12 h) most of the amides on the B-chain disappear while 11 remain on the A-chain. We have calculated the intrinsic aqueous exchange rates for each residue using the

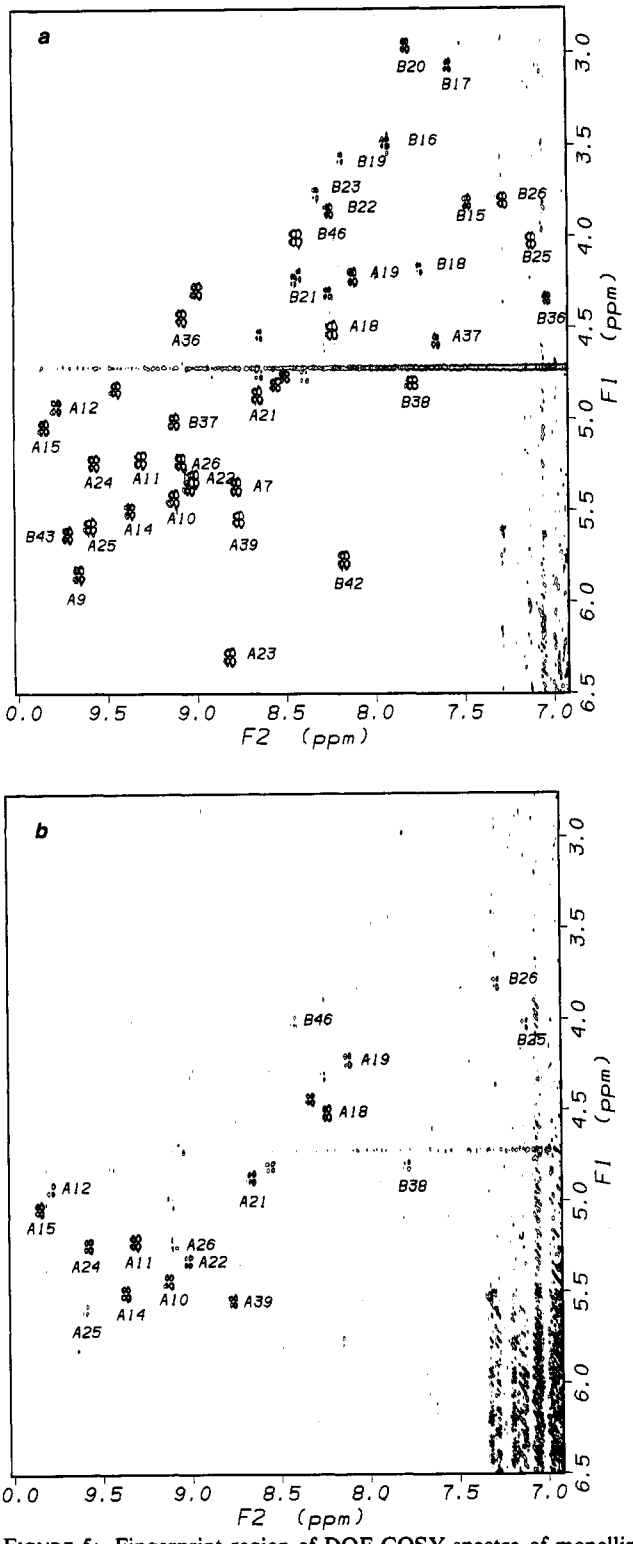

FIGURE 5: Fingerprint region of DQF COSY spectra of monellin recorded in D_2O at pH 2 and 25 °C: (a) sample freshly dissolved in D_2O; (b) sample obtained through exchange trapping experiment. After exchanging in 50% ethanol-d_6/D_2O for 6 h, the protein was renatured and redissolved in D_2O for the acquisition of the NMR spectrum. Some of the assignments are indicated (Tomic et al., 1992).

empirical rules for sequence effects (Molday et al., 1972; Robertson & Baldwin, 1991) and have confirmed that the intrinsic rates do not mirror the trends seen in the alcohol-denatured state. This suggests that the results are significant and not entirely sequence dependent. Using the assignments of Tonic et al. (1992) for native state monellin, we find that in the alcohol-denatured state the most slowly exchanging

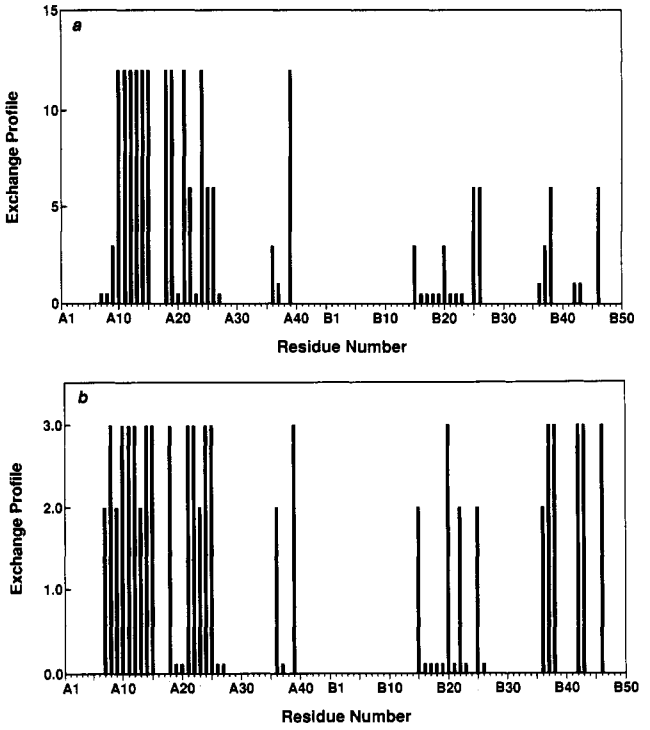

FIGURE 6: (a) Hydrogen exchange profile of monellin in 50% ethanol obtained through exchange trapping experiments. The unit for the y-axis is arbitrary and should not be compared with that of the exchange profile obtained in the native state (panel b). A value of 0 is assigned to amide protons that are rapidly exchanging in the native state. A value of 0.5 or greater is assigned to amide protons that are slow to exchange in the native state. Values of 1, 3, 6, and 12 are assigned to the amides that are observed in the native state COSY spectra after 1, 3, 6, and 12 h of exchange in 50% ethanol, respectively. (b) Hydrogen exchange profile of monellin at pH 2 in the native state. The unit for the y-axis is arbitrary and should not be compared with that of the exchange profile obtained in the alcohol denatured state (panel a). A value of 0 is given to the amides that disappear after completion of the first COSY experiment (~16 h). Values of 0.1, 2, and 3 are given to the residues that remain after the first COSY experiment, after 2 months of exchange, and after 3 months of exchange, respectively.

amide protons after 12 h include residues A10–A15, A18, A19, A21, A24, and A39. These amide protons are located primarily on one of the chains of the antiparallel β-sheet of the A-chain.

In order to interpret the hydrogen exchange kinetics, it is important to determine whether the A- and B-chains of monellin are associated and/or aggregated in alcohol. We have addressed the nature of the interactions of the A- and B-chains in alcohol by gel filtration, CD, and NMR spectroscopy. Size-exclusion chromatography shows that both monellin and the individual A-chain elute at the same volume, at a position that is consistent with the A-chain molecular weight of approximately 5000. Since the A- and the B-chains have similar molecular weights, and both are present in the eluted monellin sample, the result of the gel filtration is consistent with monellin being in a disassociated state with a mixture of monomeric A- and B-chains in solution, at the high salt concentrations required for the experiment (see Materials and Methods). Under normal saline concentrations, we obtained CD spectra of the separated A- and B-chains in TFE, ethanol, and H_2O, and compared these spectra to those of mixed A- and B-chains in the same solvents. The CD spectra of the separated A- and B-chains in TFE and in ethanol can be added to yield the spectra of monellin under the same conditions, indicating that the conformations of the A- and B-chains are independent of whether they are studied in

isolation or together. The CD spectra of the isolated A- and B-chains in H_2O cannot be added to yield native monellin indicating that the A- and B-chains are associated in H_2O. In fact, CD deconvolution indicates that the conformation of isolated A and B is largely random coil (61% and 64%, respectively). The concentration dependence of association/aggregation of monellin was studied by CD and NMR. CD molar ellipticity, NMR line widths, and NMR bulk hydrogen exchange experiments in 50% ethanol remain constant in the concentration ranges of 2 μM to 1 mM. At concentrations greater than 1 mM, the B-chain of monellin precipitates from the solution in a time-dependent manner. The high salt concentration at which the size-exclusion chromatography was run accelerates the aggregation of the B-chain over time; however, on the time scale of the gel, no aggregation was observed. The results from the gel filtration, the CD spectroscopy, and NMR indicate that monellin in alcohol is not associated/aggregated under the conditions at which the NMR experiments are performed. The implications, in terms of the hydrogen exchange trapping experiments of monellin, are that we are monitoring hydrogen exchange of the A- and B-chains independently. Chains A and B, however, cannot be studied in isolation because their random coil conformations in water cannot be used as probes to study the exchange rates in alcohol.

Hydrogen Exchange of Native-State Monellin at pH 2. We are interested in determining whether the most slowly exchanging amide protons are similar in the alcohol-denatured state and in the native state. From the hydrogen exchange trapping experiments, it was found that the most slowly exchanging regions in the alcohol-denatured state are located in the central β-sheet region of the native protein. To identify the most slowly exchanging amides in the native state, hydrogen exchange studies were undertaken. The 2D COSY spectra of the monellin in D_2O at pH 2 were taken at various time intervals, and the decay of the peak intensity was used as a semiquantitative measure of exchange. Figure 6b shows the exchange profile of native monellin at pH 2. A value of 0 is given to the amides that disappear after completion of the first COSY experiment ($\sim$16 h); values of 0.1, 2, and 3 are given to the residues that remain after the first COSY experiment, after 2 months of exchange, and after 3 months of exchange, respectively. After the first COSY experiment, there are 39 slowly exchanging amides, and after 3 months there are 18. Of the 11 slowly exchanging amide protons in the alcohol state after 12 h, 9 correspond to the most slowly exchanging protons of the native state. The most significant difference exists in the B-chain which has 6 slowly exchanging amides in the native state at long times but no slowly exchanging amides in the alcohol-denatured state.

To further confirm the fact that the two subsets of slowly exchanging amides are similar to one another and to determine if certain parts of the protein are slowly exchanging in the alcohol-denatured state but not in the native state, we have carried out the following pre-exchange experiment. The fully protonated protein was first dissolved in D_2O and left to exchange in the native state for 24 h. Ethanol-d_6 was then added to the solution, and the residual total amide intensity was monitored as a function of time. In this experiment the rapidly exchanging amide protons in the native protein ($\sim$40 residues) exchange first so that they are "invisible" in the subsequent exchange in 50% ethanol. If the slowly exchanging subset in the alcohol-denatured state is not within the slowly exchanging subset of the native state, there should be a significant difference between the two exchange curves, especially at long exchange times. The exchange curve obtained from the pre-exchange experiment and the hydrogen exchange curve obtained with freshly dissolved protein are very similar at long times. The curve fitting procedure shows that the amplitude (14) and the rate constant (6.2×10^{-4} min^{-1}) for the slow phase in the pre-exchange experiment are very similar to the amplitude (14) and rate constant (6.7×10^{-4} min^{-1}) obtained from the freshly dissolved sample (the estimated error for the amplitude and the rate constant are $\sim$20% and $\sim$10%, respectively). This implies that the majority of the observed amide protons in the alcohol-denatured state are represented within the subset of slowly exchanging protons in the native state. These results indicate that the 2D hydrogen exchange trapping experiments, in which the native state is used as a reporter of the alcohol-denatured state, can be used to represent the population of slowly exchanging amides in the alcohol-denatured state.

Preliminary NMR Assignments of Monellin A Chain in 50% TFE. Having observed the hydrogen exchange of the slowly exchanging amide protons, we would like to determine the secondary structure in the alcohol-denatured state. To resolve this question, direct NMR assignment work was carried out. In 50% ethanol the protein resonances are overlapped extensively, making direct assignment work extremely difficult. In 50% TFE, however, the resonance overlap problem is diminished. It should be emphasized that in 50% TFE the hydrogen exchange behavior is very similar to that in 50% ethanol and the CD deconvolution indicates very similar secondary structures (58% α-helix and 26% β-sheet in 50% ethanol; 57% α-helix and 19% β-sheet in 50% TFE). In addition, the hydrogen exchange trapping experiments show the same results in both solvents. Since 50% TFE offers greater chemical shift dispersion, the assignment work was carried out in this solvent. Even in 50% TFE, the NMR spectrum of monellin has severe resonance overlap due to substantial amounts of unstructured or highly dynamic regions in the protein. To further resolve this difficulty, the A- and the B-chain of monellin were isolated and studied individually. Compared with monellin (95 residues), the spectrum of the A-chain alone (45 amino acids) is considerably simplified. In addition, the A-chain is of primary interest structurally because it contains most of the slowly exchanging amide protons observed in the alcohol-denatured state. Therefore, assignments and secondary structure determination were performed on the A-chain alone.

The HN to HN region of the NOESY spectrum of the A-chain of monellin in 50% TFE/H_2O is shown in Figure 7. There is a continuous stretch of HN(i)–HN(i+1) connectivities that suggests the existence of an α-helix. The sequential assignments of this peptide segment were achieved by the combination of DQF-COSY and NOESY experiments, and the spin systems were identified with TOCSY, DQF-COSY, and NOESY experiments (Wuthrich, 1986). The complete spin systems of Ala and Thr were identified from DQF-COSY and TOCSY spectra, the AMX spin systems were identified by the fine structure of the β-protons in the DQF-COSY spectrum, and a Ser residue was identified by the unusually low-field chemical shifts of the β-protons. The Ile residues were assigned readily by their unique patterns in the DQF-COSY and TOCSY spectra, and the aromatic residues were identified by the observed NOEs between the α- and β-protons to the ring protons. From the identified spin systems and the sequential NN connectivities, the following stretch of amino acids could be identified AMX-U-U-Phe-U-Ala-AMX-Ile-Ser-Glu/Gln-AMX-Tyr-U-Thr (U denotes unidentified spin

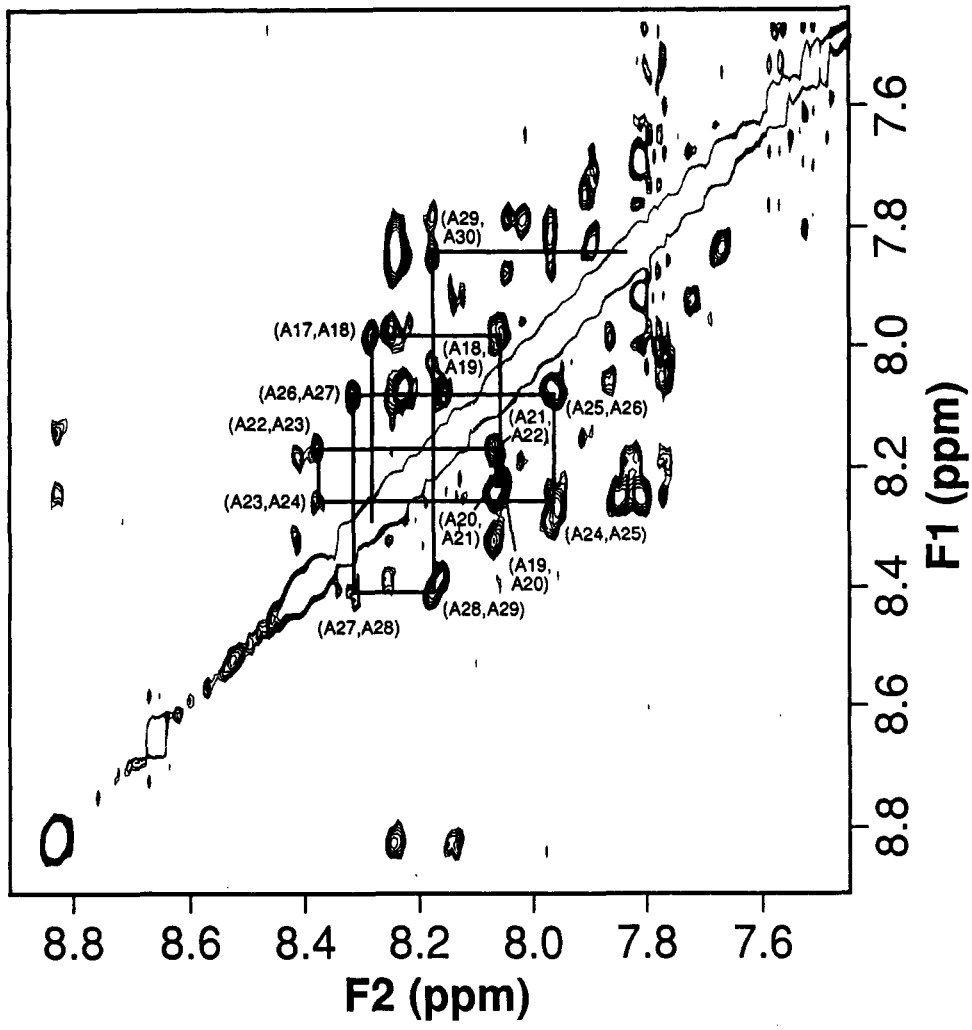

FIGURE 7: HN to HN region of the NOESY spectrum of the A-chain of monellin in 50% TFE/H_2O at pH 2 obtained with a 200-ms mixing time. The continuous stretch of HN(i) to HN(i+1) connectivities are shown and the assigned residues are labeled.

systems). This corresponds uniquely to residues 17–30 on the A-chain with the sequence Asp-Lys-Leu-Phe-Arg-Ala-Asp-Ile-Ser-Glu-Asp-Tyr-Lys-Thr. In addition to the observed HN(i)–HN(i+1) connectivities, the characteristic HCα(i)–HCβ(i+3) NOEs for α-helices were also observed between residues 17 and 20, 20 and 23, 23 and 26, 24 and 27, and 26 and 29 (Figure 8). These results strongly suggest that the peptide segment from residues 17 to 30 on the A-chain adopts an α-helical conformation in 50% TFE. An interresidue NOE between δCH_3 of Ile24 and 2,6H of Phe20 is observed but is not found in the native structure. This NOE is also consistent with the peptide being in a helical structure in 50% TFE. We should emphasize here that we have identified residues A17–A30 and have assigned this region to an α-helix. The rest of the protein in the alcohol-denatured state is very difficult to study directly, and therefore, the NMR structure is undefined.

DISCUSSION

The observed structural transition in the A-chain of monellin (residues A17–A30) from β-sheet in the native state to α-helix in the alcohol-denatured state shows that for a given amino acid sequence the environmental context in which the residues are found is an important factor in dictating the type of secondary structure adopted. This result concurs with recent studies in which β-sheet and α-helix could be induced in the same sequence by changing the solvent conditions (Zhong & Johnson, 1992; Wang et al., 1992; Zagorski & Barrow, 1992; Shibata et al., 1992). In the protein ubiquitin, CD studies in low dielectric alcohol solutions showed that the protein was mainly α-helical (Wilkinson & Mayer, 1986). More recent NMR studies of ubiquitin in methanol (Harding et al., 1991) have shown that the structure of ubiquitin is largely nativelike, in particular the β-sheet region in the native state remains in a β-sheet conformation in 60% methanol. From these studies, it is demonstrated that α-helix is not the only secondary structure that has been obtained by alcohol denaturation but that the specific structure adopted by a protein in a given solvent system is most likely determined by the primary sequence and the specific interactions between residues. It is therefore interesting to consider the secondary structure propensities of the monellin sequence. Sequence analysis of the A-chain shows that residues A17–A30 which were assigned by NMR as being in α-helix in the alcohol-denatured state correspond to a region which is predicted to be helical by the methods of Chou and Fasman (1976) and Garnier et al. (1978). Specifically, in the A-chain, the residues that are predicted to be α-helical are A1–A9, A17–A27, and A33–A38 by the Chou and Fasman (1976) method and residues A15–A26 by the method of Garnier et al. (1978). On the B-chain, residues B10–B25 are in an α-helical conformation in the native protein, and the residues that are predicted to be α-helical are residues B17–B24 by the Chou and Fasman method (1976) and B19–

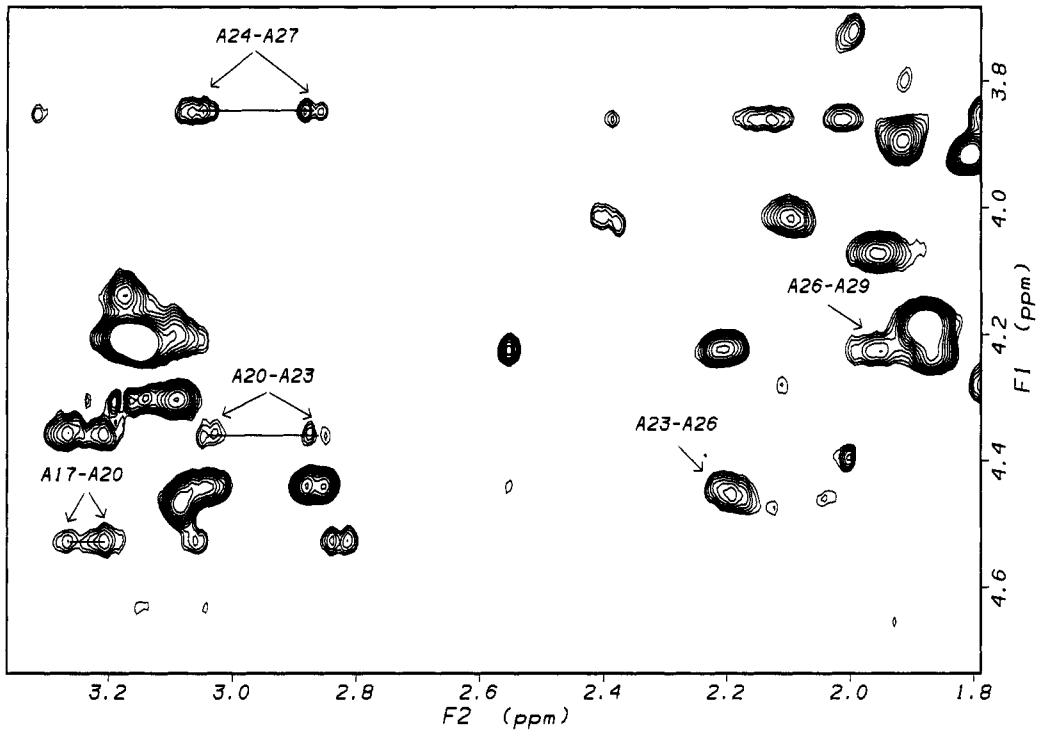

FIGURE 8: HC_α to HC_β region of the NOESY spectrum of the A-chain of monellin in 50% TFE/D_2O at pH 2 obtained with a 200-ms mixing time. The $H_{\alpha\beta}(i,i+3)$ NOE's are shown.

B24 by the method of Garnier et al. (1978). As the B-chain has not been characterized in detail by NMR, it is impossible to know whether residues B10–B25 are actually in an α-helical conformation in the alcohol-denatured state.

A number of experimental results point toward the dynamic nature of large regions of the alcohol-denatured state. The majority of the amide protons in the alcohol-denatured state exchange at rates that are comparable to the exchange rate of monellin in urea. CD spectra suggest a rather high helical content whereas only a small number of slowly exchanging amides are detected by NMR. These data suggest that large regions of the secondary structure in the alcohol-denatured state are only marginally stable and do not result in significant protection of amide protons. The loss of intensity in the near UV CD spectrum and the limited chemical shift dispersion in the NMR spectrum suggest that the tertiary interactions are nonspecific and fluctuating. This presents a picture of the alcohol-denatured state of monellin in which both the backbone and side chain residues appear to be dynamic.

Comparing the hydrogen exchange kinetics of the native and alcohol-denatured states, it is clear that many of the most slowly exchanging residues in the two states are similar. In particular, in the A-chain, the amides remaining after 2–3 months in the native state are similar to those remaining after 6–12 h in the alcohol-denatured state. However, we know that for the slowly exchanging residues A18, A19, A21, and A24, the structures in the native and alcohol-denatured states are very different. In the native state, the entire A-chain is composed of β-sheet and turns (Figure 1), and we have assigned residues A17–A30 to an α-helical conformation in the alcohol-denatured state of the A-chain. It is possible that the other slowly exchanging residues (A10–A15) on the A-chain, for which the secondary structure has not been assigned by NMR, may also occur as α-helix in the alcohol-denatured state. This is based on the hydrogen exchange pattern for residues A10–A15 and the fact that no pronounced downfield chemical shifts characteristics of β-structure are seen in the NMR spectrum, even though CD deconvolution suggests that β-sheet structure might be present in the alcohol-denatured state. The protected amide residues in the A-chain of the native state and in the A-chain of the alcohol-denatured state are similar, although the specific type of secondary structure appears to be different in the two states.

The hydrogen exchange rates of the B-chain are much faster than those of the A-chain in the alcohol-denatured state. CD deconvolution indicates that the B-chain in 50% ethanol is substantially structured and the α-helix content is estimated to be 47%, which is even higher than that of the A-chain (35%). The lack of association between the two chains indicates that the observed hydrogen exchange rates are not the result of the specific packing between the two chains. The following question then arises: what factors determine the differential hydrogen exchange rates of monellin in the alcohol-denatured state? From examination of the sequence of the A- and B-chain by hydrophobicity using the octanol to water transfer data (Fauchere & Pliska, 1983) corrected for molecular size (Sharp et al., 1991) (Figure 9), it is found that the majority of the slowly exchanging residues are hydrophobic; in particular, residues A10–A15, one of the most hydrophobic regions in the protein, are among the most slowly exchanging. Possible explanations may include preferential stabilization, in alcohols, of α-helix in hydrophobic regions. It is also possible that hydrogen exchange does not occur through a cooperative unfolding mechanism but by localized fluctuations, causing bulky hydrophobic side chains, such as tyrosine, to exclude solvent molecules more effectively.

It is interesting to note that several spectroscopic properties of the alcohol-denatured state of monellin, such as aromatic and backbone CD spectra, chemical shift dispersion, and hydrogen exchange dynamics, appear to be very similar to those of molten globule states, such as α-lactalbumin for example [for review, see Ptitsyn (1987), Kuwajima (1989), Dolgikh et al. (1981), Baum et al. (1989), and C.-L. Chyan, C. Wormald, C. M. Dobson, P. A. Evans, and J. Baum, unpublished results]. Another very similar feature of both proteins is that thermal denaturation from the alcohol-

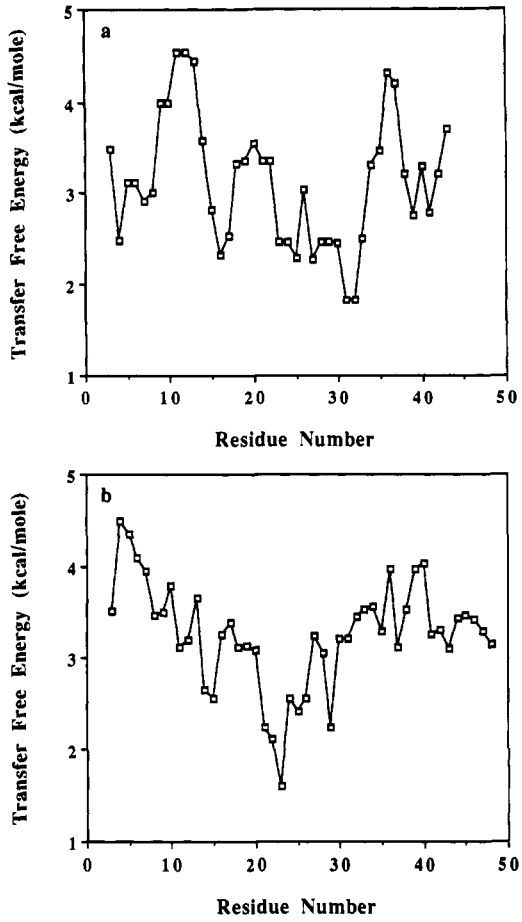

FIGURE 9: Hydrophobicity plot of (a) the A-chain of monellin and (b) the B-chain of monellin. A 5-point smoothing function was used on both data sets.

denatured and molten globule states to the unfolded state shows a very broad, almost linear transition (Pfeil et al., 1986). The differences between the alcohol-denatured and molten globule states are likely to arise in terms of the compactness of the protein. α-Lactalbumin, in the molten globule state, is known to be compact through hydrodynamic measurements (Dolgikh et al., 1981), and circumstantial evidence from NMR confirms that the molten globule state probably contains a hydrophobic core (Baum et al., 1989; C.-L. Chyan, C. Wormald, C. M. Dobson, P. A. Evans, and J. Baum, unpublished results). Monellin in the alcohol denatured state is probably not compact, as the alcohol may disrupt the hydrophobic interactions of proteins (Tanford, 1968; Timasheff & Inoue, 1968; Biringer & Fink, 1982; Zhou et al., 1992). Comparison of the two proteins suggests that alcohols may act as a good model for the hydrophobic environment of the molten globule state. For example, a small peptide fragment from α-lactalbumin is shown to have similar structure when placed in isolation in TFE and when incorporated into the protein in the molten globule state (Alexandrescu et al., 1993). An interesting implication is that since alcohol solutions do not necessarily stabilize native secondary structures, proteins in the molten globule state may contain nonnative secondary structures. These results would have important implications for protein folding mechanisms.

ACKNOWLEDGMENT

We thank Dr. David Wemmer for kindly providing us with assignments of the native monellin prior to publication. We thank Dr. Ken Breslauer for use of the CD instrument in his spectroscopy facility. We are grateful to Dr. Robert Cagan for providing us with initial monellin samples and helpful discussions. This work was supported by the Searle Scholars Fund/Chicago Community Trust.

REFERENCES

Alexandrescu, A. T., Evans, P. A., Pitkeathly, M., Baum, J., & Dobson, C. M. (1993) *Biochemistry* (in press).
Arakawa, T., & Dean, G. (1985) *Arch. Biochem. Biophys. 240*, 21–31.
Baum, J., Dobson, C. M., Evans, P. A., & Hanley, C. (1989) *Biochemistry 28*, 7–13.
Bax, A., & Davis, D. (1985) *J. Magn. Reson. 65*, 355–360.
Biringer, R. G., & Fink, A. L. (1982) *Biochemistry 21*, 4748.
Brahms, S., & Brahms, J. (1980) *J. Mol. Biol. 138*, 149–178.
Braunsweiler, L., & Ernst, R. R. (1983) *J. Magn. Reson. 53*, 521–528.
Briggs, M. S., & Roder, H. (1992) *Proc. Natl. Acad. Sci. U.S.A. 89*, 2017–2021.
Bycroft, M., Matouschek, A., Kellis, J. T., Serrano, L., & Fersht, A. R. (1990) *Nature 346*, 488–490.
Chou, P. Y., & Fasman, G. D. (1978) *Adv. Enzymol. Relat. Areas Mol. Biol. 47*, 45–148.
Dill, K. A., & Shortle, D. (1991) *Annu. Rev. Biochem. 60*, 795–825.
Dolgikh, D. A., Gilmanshin, R. I., Brazhnikov, E. V., Bychkova, V. E., Semisotnov, G. V., Venyaminov, S. Yu., & Ptitsyn, O. B. (1981) *FEBS Lett. 136*, 311–315.
Edelhoch, H. (1967) *Biochemistry 6*, 1948–1954.
Englander, S. W., & Kallenbach, N. R. (1984) *Q. Rev. Biophys. 16*, 521–655.
Evans, P. A., Topping, K. D., Woolfson, D. N., & Dobson, C. M. (1991) *Proteins: Struct., Funct., Genet. 9*, 248–266.
Fauchere, J. L., & Pliska, V. (1983) *Eur. J. Med. Chem. 18*, 369–375.
Frank, G., & Zuber, H. (1976) *Hoppe-Seyler's Z. Physiol. Chem. 357*, 585–592.
Garnier, J., Osguthorpe, D. J., & Robson, B. (1978) *J. Mol. Biol. 120*, 97–120.
Gutbezahl, B., & Grunwald, E. (1953) *J. Am. Chem. Soc. 75*, 565–574.
Harding, M. M. H., Williams, D. H., & Woolfson, D. N. (1991) *Biochemistry 30*, 3120–3128.
Hudson, G., & Biemann, K. (1976) *Biochem. Biophys. Res. Commun. 71*, 212–220.
Hughson, F. M., Wright, P. E., & Baldwin, R. L. (1990) *Science 249*, 1544–1548.
Jeng, M.-F., & Englander, S. W. (1991) *J. Mol. Biol. 221*, 1045–1061.
Jeng, M.-F., Englander, S. W., Elöve, G. A., Wand, A. J., & Roder, H. (1990) *Biochemistry 29*, 10433–10437.
Jirgenson, B. (1976) *Biochim. Biophys. Acta 446*, 255–261.
Kim, S., Kang, C. Kim, R., Cho, J. M., Lee, Y., & Lee, T. (1989) *Protein Eng. 2*, 571–575.
Kumar, A., Ernst, R. R., & Wuthrich, K. (1980) *Biochem. Biophys. Res. Commun. 95*, 1–6.
Kuwajima, K. (1989) *Proteins: Struct., Funct., Genet. 6*, 87–103.
Loftus, D., Gbenle, G. O., Kim, P. S., & Baldwin, R. L. (1986) *Biochemistry 25*, 1428–1436.
Marion, D., & Wuthrich, K. (1983) *Biochem. Biophys. Res. Commun. 113*, 967–974.
Molday, R. S., Englander, S. W., & Kallen, R. G. (1972) *Biochemistry 11*, 150–158.
Morris, J. A., & Cagan, R. H. (1972) *Biochim. Biophys. Acta 261*, 114–122.
Morris, J. A., & Cagan, R. H. (1980) *Proc. Soc. Exp. Med. 164*, 351–354.
Mueller, L., & Ernst, R. R. (1979) *Mol. Phys. 38*, 963–992.

Neri, D., Wider, G., & Wuthrich, K. (1992) *Proc. Natl. Acad. Sci. U.S.A. 89*, 4397–4401.
Ogata, C., Marcos, H., Tomlinson, G., Shin, W., & Kim, S. H. (1987) *Nature 328*, 739–742.
Otting, G., & Wuthrich, K. (1987) *J. Magn. Reson. 75*, 546–549.
Otting, G., Widmer, H., Wagner, G., & Wuthrich, K. (1986) *J. Magn. Reson. 66*, 187–193.
Pfeil, W., Bychkova, V. E., & Ptitsyn, O. B. (1986) *FEBS Lett. 198*, 287–291.
Press, W. H., Flannery, B. P., Teukolsky, S. A., & Vetterling, W. T. (1986) *Numerical Recipes*, Cambridge University Press, Cambridge.
Ptitsyn, O. B. (1987) *J. Protein Chem. 6*, 273–293.
Rance, M., Sorensen, O. W., Bodenhausen, G., Wagner, G., Ernst, R. R., & Wuthrich, K. (1983) *Biochem. Biophys. Res. Commun. 117*, 479–485.
Radford, S. E., Dobson, C. M., & Evans, P. A. (1992a) *Nature 358*, 302–307.
Radford, S. E., Buck, M., Topping, K. D., Dobson, C. M., & Evans, P. A. (1992b) *Proteins: Struct., Funct., Genet. 14*, 237–248.
Redfield, A. G., & Kunz, S. D. (1975) *J. Magn. Reson. 19*, 250–254.
Robertson, A. D., & Baldwin, R. L. (1991) *Biochemistry 30*, 9907–9914.
Roder, H., Elove, G. A., & Englander, S. W. (1988) *Nature 335*, 700–704.
Sharp, K. A., Nicholls, A., Friedman, R., & Honig, B. (1991) *Biochemistry 30*, 9686–9697.
Shibata, A., Yamamoto, M., Yamashita, T., Chiou, J.-S., Kamaya, H., & Ueda, I. (1992) *Biochemistry 31*, 5728–5733.
States, D. J., Haberkorn, R. A., & Ruben, D. J. (1982) *J. Magn. Reson. 48*, 286–292.
Tanford, C. (1968) *Adv. Protein Chem. 23*, 121–282.
Timasheff, S. N., & Inoue, H. (1968) *Biochemistry 7*, 2501–2513.
Timasheff, S. N., Townend, R., & Mescanti, L. (1966) *J. Biol. Chem. 241*, 1863–1870.
Tomic, M. T., Samoza, J. R., Wemmer, D. E., Park, Y. W., Cho, J. M., & Kim, S. H. (1992) *J. Biomol. NMR* (in press).
Udgaonkar, J. B., & Baldwin, R. L. (1988) *Nature 335*, 694–699.
Wang, J.-M., Takeda, A., Yang, J.-T., & Wu, C.-S. C. (1992) *J. Protein Chem. 11*, 157–164.
Wilkinson, K. D., & Mayer, A. N. (1986) *Arch. Biochem. Biophys. 250*, 390–399.
Wuthrich, K. (1986) *NMR of Proteins and Nucleic Acids*, Wiley, New York.
Zagorski, M., & Barrow, C. J. (1992) *Biochemistry 31*, 5621–5631.
Zhong, L., & Johnson, W. C., Jr. (1992) *Proc. Natl. Acad. Sci. U.S.A. 89*, 4462–4465.
Zhou, N. E., Zhu, B., Sykes, B. H., & Hodges, R. S. (1992) *J. Am. Chem. Soc. 114*, 4320–4326.